Int. J. Electrochem. Sci., 12 **(2017)** 10003 – 10014, doi: 10.20964/2017.11.27

International Journal of
ELECTROCHEMICAL
SCIENCE
www.electrochemsci.org

Facile Synthesis of Ni-Co LDH Nanocages with Improved Electrocatalytic Activity for Water Oxidation Reaction

Changshui Wang, Jiahui Zhang, Caiyan Shi, Dandan Cai[*]

State Key Laboratory for Chemistry and Molecular Engineering of Medicinal Resources, Ministry of Science and Technology of China; School of Chemistry and Pharmaceutical Sciences, Guangxi Normal University, Guilin, 541004, P. R. China.
[*]E-mail: caidandan86@163.com,

Received: 7 August 2017 / *Accepted:* 3 September 2017 / *Published:* 12 October 2017

The development of an inexpensive, efficient and robust water oxidation catalyst is important to achieve water splitting for renewable energy production. Herein, nickel-cobalt layered double hydroxides (Ni-Co LDHs) were rationally synthesized by a facile method and can be served as efficient electrocatalysts for water oxidation. For comparison, Ni-Co LDH nanoflowers have also been synthesized by controlling the synthetic process. The composition and morphologies of the catalysts were characterized by X-ray diffraction (XRD), field-emission scanning electron microscopy (FESEM) and X-ray photoelectron spectroscopy (XPS). The as-obtained Ni-Co LDH nanocages exhibit a high catalytic activity toward the water oxidation reaction (WOR). The electrochemical results show that the overpotential of Ni-Co LDH nanocages electrode was 350 mV at a catalytic current density of 10.0 mA cm^{-2} in 1.0 M KOH. Moreover, the Tafel slope was as low as ~ 93 mV dec^{-1}. The unusual catalytic properties of Ni-Co LDH nanocages could be attributed to the hollow structure and the synergetic effect between Ni metal and Co metal.

Keywords: Ni-Co LDH; nanocages; ZIF-67; electrocatalysis; water oxidation

1. INTRODUCTION

The urgent need for renewable energy sources that avoid carbon dioxide emission has forged research in different directions and water splitting is regarded as an ideal route to meet this demand [1]. The splitting of water is an oxidation-reduction reaction, where reduction produces H_2 and oxidation produces O_2. The latter has been considered to be more important and more challenging reaction, because it can provide both electrons and protons for the generation of hydrogen and involve a multi-electron transfer process. The suitable water oxidation catalysts (WOCs) are required to lower

the driving potential ($2H_2O \rightarrow O_2\uparrow+4H^+ +4e^-$) [2]. A series of complexes and metal oxides of ruthenium and iridium have been developed as WOCs [3]. Although they show great water oxidation catalytic activities, their practical application may be significantly hampered because of their low abundance and high cost [4, 5]. Therefore, it is of considerable interest and great significance to develop the robust, efficient and inexpensive WOCs.

Up to now, various transition metal oxides, oxyhydroxide, phosphides, sulfides, polyoxometalates and metal-organic complexes have been exploited as promising electrocatalysts for water oxidation [6-11]. Particularly in recent years, the bimetal layered double hydroxides (LDHs) have been attracted considerable attention due to the flexible tunability of metal cations in the layers and the facile exchangeability of intercalated anions [12-14]. Although Ni- and Co-containing materials have been considered as versatile candidates for electrocatalytic WOR, the study for Ni-Co LDH seems to be overlooked [15-19]. It is expected that Ni-Co LDH would be a promising WOC because the Ni and Co coexisting systems may further provide synergistic effect on the electrocatalysis and their special layer structural features. Generally, the conventional methods for preparation of Ni-Co LDHs mainly include co-precipitation, ion-exchange and hydrothermal methods [20-23]. In addition, it has been well accepted that hollow nanostructures could be beneficial to the electrochemical performance for WOR due to the intriguing features such as rich electroactive sites, the permeability of electrolyte and the increased surface area [24-26]. However, the above-mentioned methods might result difficult-to-control the morphology, the size distribution, surface area *et al,* and significantly limiting their potential performance gain for WOR. So, developing facile synthetic method to obtain Ni-Co LDH hollow nanoarchitectures with delicate morphologies is urgently needed. Recently, zeolitic imidazolate frameworks (ZIFs) have proved to be ideal templates and versatile precursors for the preparation of various nanomaterials due to their controllable porous structures and adjustable compositions [9, 20, 26, 28]. What's more, self-sacrificed templates tend to be good choices for fabricating various nanomaterials with hollow structures. Notwithstanding many nanomaterials with hollow structures have been developed using ZIF-67 as template, to the best of our knowledge, the Ni-Co LDHs with hollow structures as electrocatalytic WOCs have not been well explored yet.

Inspired by the above considerations, Ni-Co LDH nanocages were successfully prepared by a facile and simple method using ZIF-67 as both sacrificial template and Co source. The microstructures, morphologies and the oxidation state of Ni-Co LDH were characterized by XRD, FESEM and XPS. As expected, the Ni-Co LDH nanocages exhibited enhanced electrocatalytic performances in terms of low overpotential, high current density and stabilities for WOR compared to those of Ni-Co LDH nanoflowers.

2. EXPERIMENTAL SECTION

2.1. Materials

Cobalt nitrate hexahydrate ($Co(NO_3)_2 \cdot 6H_2O$), Nickel nitrate hexahydrate ($Ni(NO_3)_2 \cdot 6H_2O$), 2-Methylimidazole and potassium hydroxide were purchased from aladdin Chemical Reagent Co. Ltd.

Nafion solution (5 wt %) were purchased from DuPont Co. Ltd. Absolute ethanol and methanol was obtained from Xilong Chemical Reagent Co. Ltd. All chemicals were analytically pure and were used without further purification. ITO glass (R_s <6 Ohms) was purchased from Shenzhen south china Xiang city technologies Co., Ltd.

2.2. Syntheses of Compounds

2.2.1 Synthesis of ZIF-67 nanocrystals.

ZIF-67 samples were prepared according to a previously reported route [29]. Typically, 1.74 g of $Co(NO_3)_2 \cdot 6H_2O$ and 3.93 g of 2-methylimidazole were dissolved in 100 mL of methanol solution, respectively. The latter solution was quickly added into the former solution under vigorous stirring. Then, the resultant mixed solution was aged at room temperature for 24 h and the obtained purple product was collected by centrifugation and washed with methanol three times. Finally, the product was dried in vacuum at 80 ^oC for 8 h.

2.2.2 Synthesis of Ni-Co LDH nanocages

First, ZIF-67 templates (80 mg) was dispersed in 50 mL ethanol containing $Ni(NO_3)_2 \cdot 6H_2O$ (160 mg). Then the above mixture was stirred for 30 min, washed with ethanol by centrifugation and dried at 70 °C to form the ZIF-67@Ni-Co LDH. Next, 40 mg of ZIF-67@Ni-Co LDH was first dispersed in a mixed solvent consisting of 20 mL of ethanol and 5 mL of water. Then the mixed solution was refluxed at 90 °C for 1 h, during which time the ZIF-67 template can be completely removed. Finally, the yellow-green product was washed by ethanol for several times and dried at 70 ^oC for 10 h.

2.2.3 Synthesis of Ni-Co LDH nanoflowers

ZIF-67 templates (80 mg) was transferred into a round bottom flask containing $Ni(NO_3)_2 \cdot 6H_2O$ (160 mg), 10 mL of ethanol and 15 mL of water. Then the mixture was refluxed for 1 h at 90 °C under stirring. Finally, the blue-green powders were collected by centrifugation, washed with ethanol, and dried at 70 °C.

2.3. Electrochemical measurements

Firstly, 2 mg of the Ni-Co LDH nanomaterials was mixed with 0.18 mL of ethanol and 0.02 mL of 5 wt% nafion solution by sonication 30 min to form the catalyst ink. Then, 3 μL of the ink was drop-casted onto a 3 mm in diameter glassy carbon electrode (GCE) and left to dry in air, yielding a catalyst loading of ~0.42 mg cm^{-2}. Prior to the tests, GCEs was polished on a polishing cloth with Al_2O_3 powders of different grain size (1-0.05 μm) and cleaned by ultrasonication in millipore water,

ethanol and deionized water for 10 minutes successively. The catalytic activity was measured in a standard three-electrode system at 25 ^{o}C with an electrochemical analyzer (760E CH Instrument, purchased from Shanghai Chenhua Instrument Co., Ltd.). The reference electrode and counter electrode were an Ag/AgCl electrode (3 M KCl, 0.206 V *vs.* RHE) and Pt wire, respectively. The GCEs with the Ni-Co LDH nanomaterials were used as working electrodes.

The linear sweep voltammograms (LSV) were carried out at a scan rate of 5 mV/s in 1.0 M potassium hydroxide (KOH). There was an iR drop for compensation were used for the LSV test. All the measured potentials in this study were converted to reversible hydrogen electrode (RHE) with the Nernst equation: $E_{vs.RHE} = E_{vs.Ag/AgCl} + 0.059\times pH + 0.206$ V. The overpotential (η) was obtained according to the following the formula: $\eta = E_{vs.RHE}-1.23$ V. The Tafel slope was calculated according to the Tafel equation: $\eta = b\log j + a$, where η is the overpotential, b is the Tafel slope, and j is the corresponding current density.

The chronopotentiometry to evaluate the stability of the catalysts was recorded at a constant current density of 10.0 mA cm^{-2} without iR compensation. The Ni-Co LDH catalysts were deposited on ITO slides (1 cm × 2.5 cm, exposed surface area 0.5 cm^2) by controlled drop casting method. The ITO electrode was cleaned prior use by sonication for 10 minutes in ethanol and deionized water successively and dried in air.

2.4. Structural characterization

The crystal structures of the as-prepared materials were determined by X-ray diffraction (XRD, Cu Kα, λ = 1.54056 Å) with a Rigaku D/max-IIIA diffractometer at 293 K. the morphology and microstructure were characterized by field-emission scanning electron microscopy (FESEM, Quanta 200 FEG). The FESEM samples were prepared by dropping an ethanol suspension of the as-prepared samples on a silicon wafer, which were dried in air. Surface composition and valence state of metal elements were investigated by the X-ray photoelectron spectroscopy (XPS, ESCALAB250) instrument, using a 150 W Al *Kα* excitation source at 1486.6 eV. To further confirm the relative molar ratio of the metal in the bimetallic LDH, inductively coupled plasma-mass spectroscopy (ICP-MS) analysis was carried out on a Perkin-Elmer NexION300 spectrometer.

3. RESULTS AND DISCUSSION

3.1. Microstructure characterization

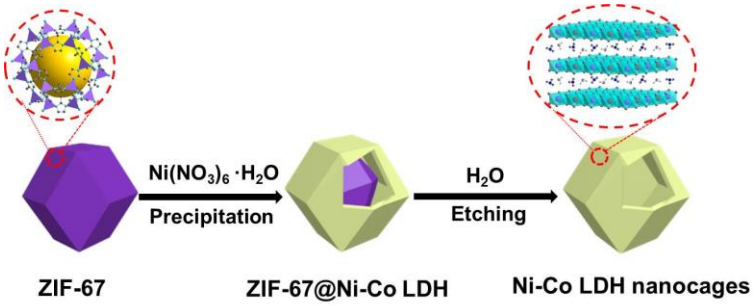

Figure 1. Schematic illustration of the formation process of Ni-Co LDH nanocages.

The detailed synthesis process of the Ni-Co LDH nanocages is schematically shown in Figure 1. Firstly, Co-based zeolitic imidazolate frameworks (ZIF-67) with rhombic dodecahedral shape were synthesized by mixing $Co(NO_3)_2 \cdot 6H_2O$ and 2-methylimidazole in methanol with the mixture being aged for 24 h [29]. Then the as-obtained ZIF-67 nanopolyhedra are reacted with $Ni(NO_3)_2 \cdot 6H_2O$ to generate Ni-Co LDH on the surface of ZIF-67 nanopolyhedra (denoted as ZIF-67@Ni-Co LDH). During the process, hydrolysis of Ni^{2+} ions can generate protons and nickel hydroxide. The as-obtained protons can etch ZIF-67 templates, which results in the release of Co^{2+} ions. The Co^{2+} and Ni^{2+} ions might be partially oxidized to Co^{3+} and Ni^{3+} by NO^{3-} ions and dissolved O_2 in the solution [8, 20, 26]. Then Ni-Co LDH was obtained by the co-precipitation of the hydroxide ions, trivalent and divalent metal. The ZIF-67 outside part of the nanopolyhedra was chemically converted into Ni-Co LDH to form ZIF-67@LDH with yolk-shelled structure by controlling the reaction time and temperature. Finally, ZIF-67 could be more easily removed by refluxing in a mixed solvent of ethanol and water at 90 ^oC [26]. Note that ethanol was chosen as the part of the mixed solvent to slow down the dissolution of ZIF-67, preventing collapse of hollow structure. As a result, the unique hollow Ni-Co LDH nanocages were successfully obtained. To demonstrate the importance of the hollow structure features for high-performance water oxidation, Ni-Co LDH nanoflowers were prepared by directly refluxing of ZIF-67 and $Ni(NO_3)_2 \cdot 6H_2O$ in the mixed solvent of water and ethanol.

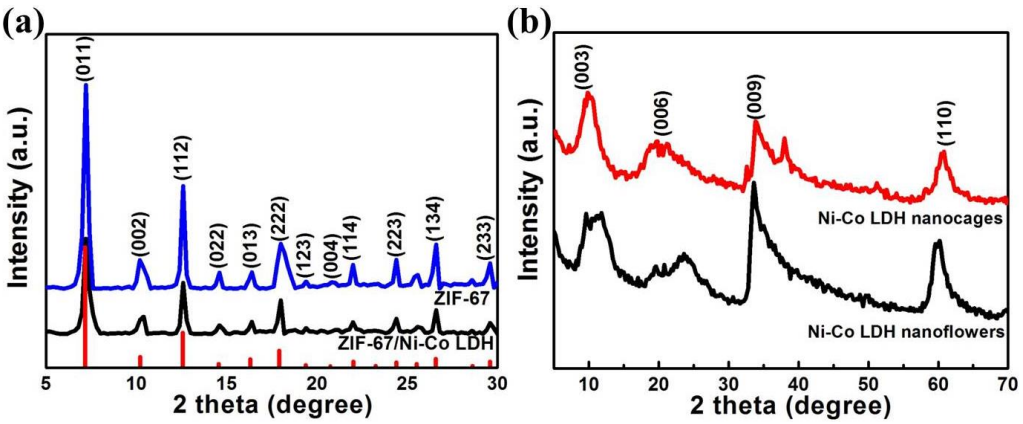

Figure 2. XRD patterns of (a) ZIF-67 and ZIF-67@Ni-Co LDH nanocrystals, (b) Ni-Co LDH nanocages and Ni-Co LDH nanoflowers.

Figure 2a shows the XRD patterns of ZIF-67 and ZIF-67@Ni-Co LDH nanocrystals. The diffraction peaks of ZIF-67 template matches well with the previously reported patterns, demonstrating that the as-obtained templates are phase-pure [8, 9, 20, 26, 29]. In addition, the XRD patterns of ZIF-67@Ni-Co LDH are consistent with that of ZIF-67, suggesting that ZIF-67 has a more distinct crystal structure than Ni-Co LDH [8, 26]. As shown in Figure 2b, five characteristic diffraction peaks at about 12^o, 22^o, 33^o, 39^o and 60^o are clearly observed. The above diffraction peaks could be attributed to the (003), (006), (009), (015) and (110) plane reflections of the hydrotalcite-like LDH phase [21-23]. The results indicated that Ni-Co LDH could be successfully prepared by using the rhombic dodecahedral ZIF-67 as sacrificial templates. It should be pointed out the diffraction peak of Ni-Co LDH

nanoflowers at 39^{o} is disappeared compared with that of Ni-Co LDH nanocages. The major reason of this phenomenon might be the different ratio of nickel and cobalt in the Ni-Co LDH [20, 26].

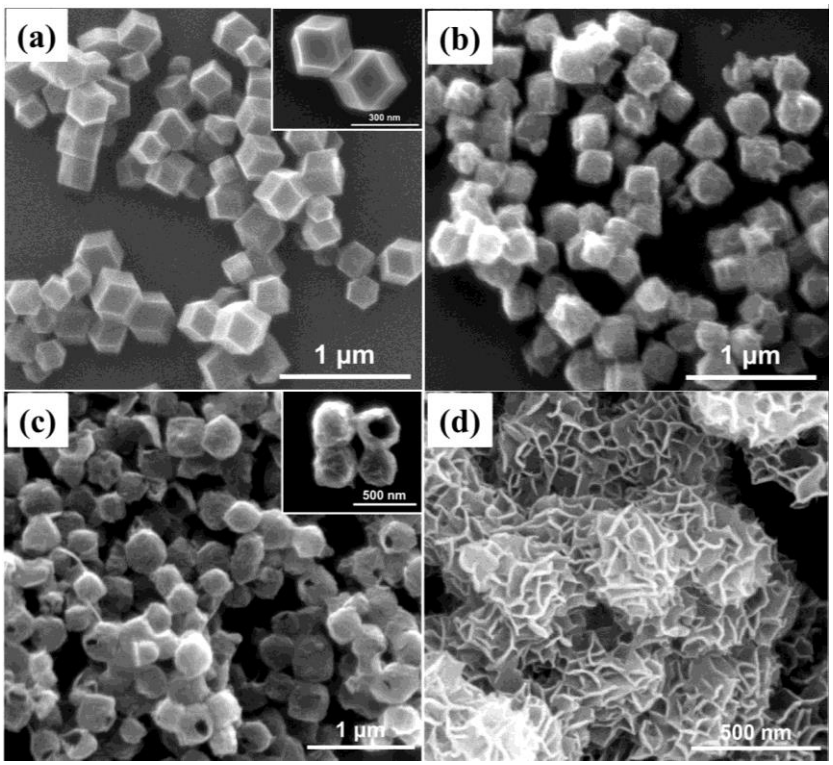

Figure 3. FESEM images of (a) ZIF-67, (b) ZIF-67@Ni-Co LDH nanocrystals, (c) Ni-Co LDH nanocages and (d) Ni-Co LDH nanoflowers.

The morphology of the ZIF-67 and ZIF-67@Ni-Co LDH nanocrystals is characterized by FESEM. From Figure 3a, the ZIF-67 particles show a rhombic dodecahedron shape, which is like that of ZIF-67 previously reported [8, 9, 20, 26, 29]. Moreover, the obtained ZIF-67 nanopolyhedra are uniform with a size of about 300 nm. A higher magnification FESEM image (inset in Figure 3a) reveals that the surfaces of ZIF-67 nanocrystals are smooth. After reacting with $Ni(NO_3)_2 \cdot 6H_2O$ at room temperature, the shapes of the particles are converted into nanoboxes from nanopolyhedra and exhibit a rougher surface (Figure 3b). As shown in Figure 3c, FESEM images of the particles show cage-like structures. The broken outer shells reveal fully hollowed Ni-Co LDH nanocages, indicating that was complete removal of the ZIF-67 templates. What's more, the Ni-Co LDH nanocages show mild shrinkage with decreased average size of about 250 nm compared with the ZIF-67 templates. For comparison, Ni-Co LDH nanoflowers were obtained by adjusting the synthestic process. From Figure 3d, the nanoflowers were composed of the interconnected and thin nanosheets without hollow structure.

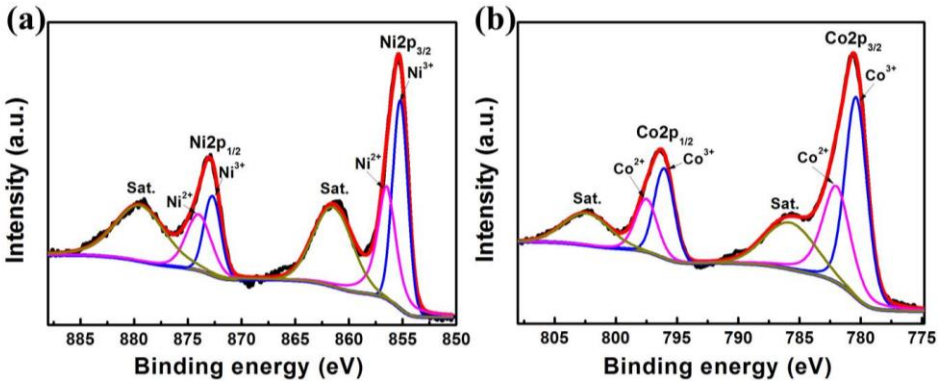

Figure 4. (a) Ni 2p and (b) Co 2p XPS spectra of Ni-Co LDH nanocages.

The detailed chemical states and surface compositions of Ni-Co LDH nanocages were further analyzed by XPS, as shown in Figure 4. The Co 2p and Ni 2p spectra of the Ni-Co LDH are split into $2p_{3/2}$ and $2p_{1/2}$ doublets due to spin-orbit coupling. The two obvious cobalt species of Co 2p at 780.4 eV and 796.1 eV can be identified as Co $2p_{3/2}$ and Co $2p_{1/2}$ of Co^{3+}, respectively. Meanwhile, another two fitting peaks at 782.1 and 797.6 eV are assigned to Co^{2+} [19, 22]. The peak analysis (Figure 4a) of Ni 2p for Ni-Co LDH nanocages shows two kinds of nickel species, which can be identified at Ni^{2+} ($2p_{3/2}$ and $2p_{1/2}$ at 855.2 eV and 872.7 eV, respectively) and Ni^{3+} ($2p_{3/2}$ and $2p_{1/2}$ at 856.5 and 874.0 eV, respectively) [22, 23]. Therefore, it could be demonstrated the co-existence of multiple valence state for Co and Ni in Ni-Co LDH nanocages. Moreover, it is reasonably expected that the solid-state redox couples of Co^{2+}/ Co^{3+} and Ni^{2+}/Ni^{3+} in Ni-Co LDH nanocages might provide excellent electrochemical properties, because metal cations with mixed-valence have been considered as the catalytically active centres for WOR [30, 31]. In addition, the surface atomic ratio of Ni to Co in the Ni-Co LDH nanocages is approximately 5:7, which is consistent with the result of ICP-MS (27:35), suggesting that the Ni and Co are evenly distributed in the nanomaterials.

3.2. Electrocatalytic properties of the Ni-Co LDH nanocages and Ni-Co LDH nanoflowers

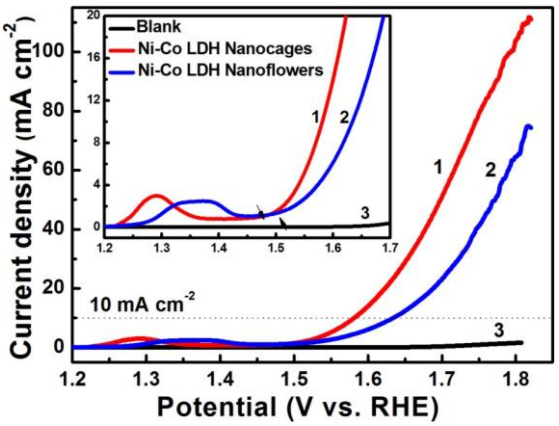

Figure 5. Polarization curves of the (1) Ni-Co LDH nanocages, (2) Ni-Co LDH nanoflowers and (3) blank for WOR in 1.0 M KOH solution at a scan rate of 5 mV s^{-1}, The inset shows the magnified view of the polarization curves.

The electrocatalytic activities of the Ni-Co LDH nanocages and Ni-Co LDH nanoflowers toward the WOR were investigated by measuring LSV in alkaline solution using a typical three-electrode system. Fgiure 5 shows the polarization curves for WOR about different catalysts (Ni-Co LDH nanocages and Ni-Co LDH nanoflowers) in 1.0 M KOH solution at a scan rate of 5 mV s^{-1}. The two LDH modified electrodes were prepared by droping catalytic ink solutions on GCE. Both the two Ni-Co LDH modified electrodes exhibited catalytic activities, which could be attributed to the similar layer structures. As shown in Figure 5, the Ni-Co LDH nanocages are highly active for the WOR. The Ni-Co LDH nanocages could approach a large current density of 111 mA cm^{-2} at an overpotential of 570 mV, which is much better than that of Ni-Co LDH nanoflowers (74 mA cm^{-2}). Moreover, the onsetpotential of the Ni-Co LDH nanocages electrodes for WOR is the lowest at ~1.48 V (*vs.* RHE) compared to Ni-Co LDH nanoflowers (~1.51 V *vs.* RHE) electrodes (inset in Figure 5). This low onset overpotential (250 mV) for Ni-Co LDH nanocages electrodes is favorably comparable to or even lower than those previously reported for Co or Ni-based hydroxides catalysts, such as Ni-Co LDH nanosheets on nickel foam (290 mV) [22], exfolited NiCo LDH nanosheets on carbon paper (280 mV) [23] and Co-Ni LDH on fluorine doped tin oxide over-layer (FTO) (393 mV) [32]. Meanwhile, the catalytic current for Ni-Co LDH nanocages modified electrode increased more rapidly than those for Ni-Co LDH nanoflowers electrodes after 1.50 V *vs.* RHE. In addition, the GCE also was tested as control samples under the same conditions. In Figure 5, polarization curve of blank GCE (black plot) revealed no oxidative catalytic current, suggesting the efficient catalytic roles of the two Ni-Co LDH nanomaterials in the WOR process. Note that an anodic peak of 1.36 V *vs.* RHE for Ni-Co LDH nanoflowers is observed, which is assigned to the M^{2+}/M^{3+} transformation (M=Ni and Co) [11, 16, 22, 23]. For Ni-Co LDH nanocages electrodes, the anodic peak was shifted toward negative direction (1.29 V vs RHE), due to the good wettability of electrolyte and many active sites in hollow structure [6, 9, 25-27].

Furthermore, it was observed that an overpotential (η) of 400 mV was needed to generate an anodic current density of 10.0 mA cm^{-2} for Ni-Co LDH nanoflowers. In contrast, Ni-Co LDH nanocages exhibited better performance for electrocatalytic water oxidation, achieving current densities of 10.0 mA cm^{-2} at 1.58 V vs. RHE (η = 350 mV). Impressively, the catalytic activity can be also competitive with those of noble-metal-free Ni-based and Co-based WOCs, such as the nanostructured α-nickel-hydroxide (331 mV for 10 mA cm^{-2}) [16] and the mesoporous Co_3O_4 spinels (411 mV for 10 mA cm^{-2}) [33]. Moreover, the overpotential was even lower than that of the previous reported commercial RuO_2 catalyst (371 mV for 1.0 mA cm^{-2}) [34] and Ir/C catalyst (409 mV for 10 mA cm^{-2}) [33]. Therefore, Ni-Co LDH nanocages show a high catalytic activity in term of lower overpotential and larger catalytic current density for water oxidation.

A Tafel plot reflects the electrochemical kinetics through the relation of the elecatrcatalytic current density and the overpotential [22-26]. So the WOR kinetics of the two LDH electrodes were estimated by the corresponding Tafel plots. The Tefel plots for Ni-Co LDH nanocages and Ni-Co LDH nanoflowers electrodes films in 1.0 M KOH were obtained by measuring the current densities as a function of the overpotential (η). As shown in Figure 6, the Ni-Co LDH nanocages exhibit a lower Tafel slope of 93 mV dec^{-1} than Ni-Co LDH nanoflowers (142 mV dec^{-1}). The results indicate that the WOR kinetics for Ni-Co LDH nanocages is more favorable that the Ni-Co LDH nanoflowers samples.

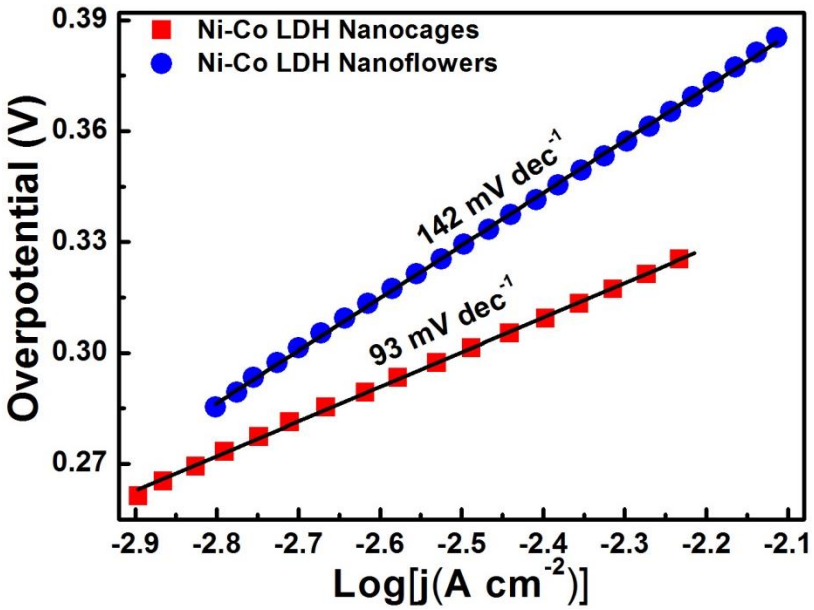

Figure 6. Tafel plots of the Ni-Co LDH nanocages and Ni-Co LDH nanoflowers for WOR in 1.0 M KOH solution.

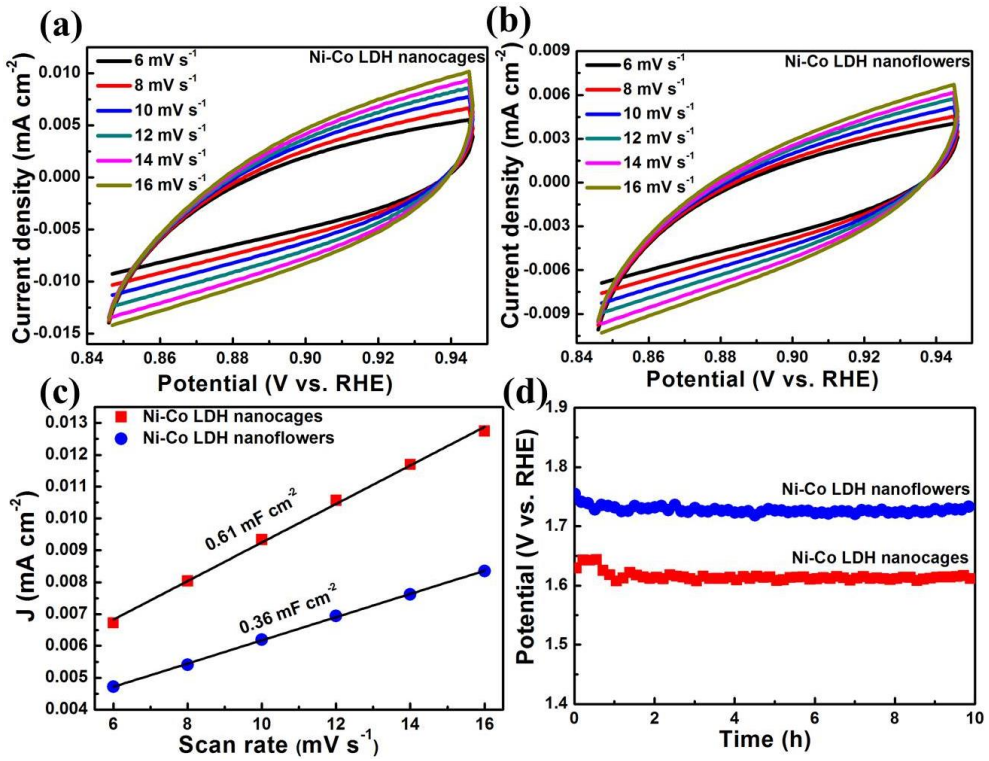

Figure 7. Cyclic voltammetry (CV) curves for (a) Ni-Co LDH nanocages and (b) Ni-Co LDH nanoflowers at scan rates of 6, 8, 10, 12, 14 and 16 mV s^{-1} in 1.0 M KOH solution; (c) Charging current density differences ($J=J_a-J_c$) plotted against scan rates; (d) Representative chronopotentiometry data for the two Ni-Co LDH on ITO electrodes with a fixed catalytic current density of 10.0 mA cm^{-2} without iR compensation.

It is believed that the electrochemical double-layer capacitance (C_{dl}) is linearly proportional to the electrochemically active surface areas (ECSA) and the linear slope is equivalent to twice of the C_{dl} [22, 23]. To compare ECSA of the two LDH nanomaterials, the C_{dl} of the Ni-Co LDH nanocages and Ni-Co LDH nanoflowers were determined by measuring the CV curves in a non-faradaic region from 0.846 to 0.946 V *vs.* RHE. Figure 7a, 7b and 7c shows the CV curves for Ni-Co LDH nanocages and nanoflowers in 1.0 M KOH solution and the plots of $J=J_a-J_c$ at 0.896 V *vs.* RHE against the scan rates. Evidently, the slope of the Ni-Co LDH nanocages is much larger than the Ni-Co LDH nanoflowers, revealing the higher active surface area of Ni-Co LDH nanocages. The comparison might provide some explanation for the much enhanced electrocatalytic performance for Ni-Co LDH nanocages with hollow structures. What's more, the result is consistent with the comparison of the above-mentioned Tafel slopes.

Besides the catalytic activity, stability represents another important criterion for evaluating electrocatalysts in practical applications [8, 22-24]. In order to further confirm the stability of the Ni-Co LDH during water oxidation catalytic process, these two LDHs nanomaterilas were deposited on ITO electrodes (to prevent the falling of sample off substrate) and chronopotentiometry experiment was performed at a constant current density (10.0 mA cm^{-2}) in 1.0 M KOH. As shown in Figure 7d, there was no significant decay of the catalytic currents observed during 10 h of electrolysis, suggesting the Ni-Co LDH nanocages and Ni-Co LDH nanoflowers have excellent stability under continuous operation in alkaline solution. At a fixed current density of 10.0 mA cm^{-2} for the Ni-Co LDH nanocages, a stable potential of about 1.63 V *vs.* RHE is observed, which is lower than that (1.74 V *vs.* RHE) of Ni-Co LDH nanoflowers. The result further indicated that nanocages with hollow structure could enhance the activity of water oxidation reaction.

4. CONCLUSIONS

In summary, the Ni-Co LDH nanocages were successfully prepared by a facile method and studied as highly active electrocatalysts for water oxidation. The as-obtained Ni-Co LDH nanocages was achieved a catalytic current density of 10.0 mA cm^{-2} at a quite low overpotential of 350 mV. Moreover, the low onset potential is 1.48 V *vs.* RHE and the low Tafel slope is about 93 mV dec^{-1}. The results indicate that the Ni-Co LDH nanocage is a promising and excellent candidate of water oxidation catalyst made up of nonprecious metal elements. The facile method might drive the development of preparation other bi-metal LDH nanomaterials with hollow structure. Furthermore, the efficient catalytic properties of Ni-Co LDH nanocages will expand the application of LDH in electrocatalytic field.

ACKNOWLEDGEMENTS

This work was financially supported by the National Natural Science Foundation of China (No. 21661008, 21371037), the Natural Science Foundation of Guangxi Province (No. 2015GXNSFBA139025, 2014GXNSFFA118003), BAGUI scholar program (2014A001), the project

of talents highland of Guangxi province, the Science and Technology Research Project of Guangxi Universities (No. KY2015YB035) and the Program for Key Scientific Research of Guangxi Normal University (2014ZD006).

References

1. A. Singh and L. Spiccia, *Coordin. Chem. Rev.*, 257 (2013) 2607.
2. P. Du and R. Eisenberg, *Energy Environ. Sci.*, 5 (2012) 6012.
3. M. D. Karkas, O. Verho, E. V. Johnston and B. Akermark, *Chem. Rev.*, 114 (2014) 11863.
4. J. R and G. Mascarós, *ChemElectroChem*, 2 (2015) 37.
5. L. Han, S. Dong and E. Wang, *Adv. Mater.*, 28 (2016) 9266.
6. X. Gao, H. Zhang, Q. Li, X. Yu, Z. Hong, X. Zhang, C. Liang and Z. Lin, *Angew. Chem. Int. Ed.*, 55 (2016) 6290.
7. L. Trotochaud, S. L. Young, J. K. Ranney and S. W. Boettcher, *J. Am. Chem. Soc.*, 136 (2014) 6744.
8. P. He, X. Y. Yu and X. W. Lou, *Angew. Chem. Int. Ed.*, 56 (2017) 3897.
9. Y. Guo, J. Tang, H. Qian, Z. Wang and Y. Yamauchi, *Chem. Mater.*, 29 (2017) 5566.
10. Q. Yin, J. M. Tan, C. Besson, Y. V. Geletii, D. G. Musaev, A. E. Kuznetsov, Z. Luo, K. I. Hardcastle and C. L. Hill, *Science*, 328 (2010) 342.
11. S. Zhao, Y. Wang, J. Dong, C. T. He, H. Yin, P. An, K. Zhao, X. Zhang, C. Gao, L. Zhang, J. Lv, J. Wang, J. Zhang, A. M. Khattak, N. A. Khan, Z. Wei, J. Zhang, S. Liu, H. Zhao and Z. Tang, *Nat. Energy*, 1 (2016) 16184.
12. M. Shao, R. Zhang, Z. Li, M. Wei, D. G. Evans and X. Duan, *Chem. Commun.*, 51 (2015) 15880.
13. G. Fan, F. Li, D. G. Evans and X. Duan, *Chem. Soc. Rev.*, 43 (2014) 7040.
14. R. Liu, Y. Wang, D. Liu, Y. Zou and S. Wang, *Adv Mater.*, (2017) 1701546.
15. T. Sun, L. Xu, Y. Yan, A. A. Zakhidov, R.H. Baughman and *J. Chen, ACS Catal.*, 6 (2016) 1446.
16. M. Gao, W. Sheng, Z. Zhuang, Q. Fang, S. Gu, J. Jiang and Y. Yan, *J. Am. Chem. Soc.*, 136 (2014) 7077.
17. M. Pramanik, C. Li, M. Imura, V. Malgras, Y. M. Kang and Y. Yamauchi, *Small*, 12 (2016) 1709.
18. J. Yu, Q. Li, Y. Li, C. Y. Xu, L. Zhen, V. P. Dravid and J. Wu, *Adv. Funct. Mater.*, 26 (2016) 7644.
19. H. Cheng, Y. Z. Su, P. Y. Kuang, G. F. Chen and Z. Q. Liu, *J. Mater. Chem. A*, 3 (2015) 19314.
20. Z. Jiang, Z. Li, Z. Qin, H. Sun, X. Jiao and D. *Chen, Nanoscale*, 5 (2013) 11770.
21. H. Chen, L. Hu, M. Chen, Y. Yan and L. Wu, *Adv. Funct. Mater.*, 24 (2014) .
22. J. Jiang, A. Zhang, L. Li and L. Ai, *J. Power Sources*, 278 (2015) 445.
23. H. Liang, F. Meng, M. C. Acevedo, L. Li, A. Forticaux, L. Xiu, Z. Wang and S. Jin, *Nano Lett.*, 15 (2015) 1421.
24. C. Zhang, M. Shao, L. Zhou, Z. Li, K. Xiao and M. Wei, *ACS Appl. Mater. Inter.*, 8 (2016) 33697.
25. J. Zhang, Y. Yang, Z. Zhang, X. Xu and X. Wang, *J. Mater. Chem. A*, 2 (2014) 20182.
26. H. Hu, B. Guan, B. Xia and X. W. Lou, *J .Am. Chem. Soc.*, 137 (2015) 5590.
27. Z. Lv, Q. Zhong, and Y. Bu, *Electrochim. Acta*, 215 (2016) 500.
28. M. Zhang, Y. L. Huang, J. W. Wang and T. B. Lu, *J. Mater. Chem. A*, 4 (2016) 1819.
29. W. Xia, J. Zhu, W. Guo, L. An, D. Xia and R. Zou, *J. Mater. Chem. A*, 2 (2014) 11606.
30. A. M. Ullman, Y. Liu, M. Huynh, D. K. Bediako, H. Wang, B. L. Anderson, D.C. Powers, J. J. Breen, H. D. Abruna and D. G. Nocera, *J. Am. Chem. Soc.*, 136 (2014) 17681.
31. J. H. Xu, L. Y. Guo, H. F. Su, X. Gao, X. F. Wu, W. G. Wang, C. H. Tung and D. Sun, *Inorg. Chem.*, 56 (2017) 1591.
32. Y. Zhang, B. Cui, C. Zhao, H. Lin and J. Li, *Phys. Chem. Chem. Phys.*, 15 (2013) 7363.
33. Y. J. Sa, K. Kwon, J. Y. Cheon, F. Kleitz and S. H. Joo, *J. Mater. Chem. A*, 1 (2013) 9992.
34. T. Sun, L. Xu, Y. Yan, A. A. Zakhidov, R. H. Baughman and *J. Chen, ACS Catal.*, 6 (2016) 1446.

35. C. Wang, Y. Sui, G. Xiao, X. Yang, Y. Wei, G. Zou and B. Zou, *J. Mater. Chem. A*, 3 (2015) 19669.
36. Y. Zhang, Q. Shao, Y. Pi, J. Guo and X. Huang, *Small*, 13 (2017) 1700355.